Hydride Fluxionality in Transiton Metal Complexes: An Approach to the Understanding of Mechanistic Features and Structural Diversities

Dmitry G. Gusev and Heinz Berke*

Anorganisch-Chemisches Institut, Universität Zürich,
Winterthurerstraße 190, CH-8057 Zürich, Switzerland

Received April 26, 1996

Key Words: Fluxionality, hydride / Hydride fluxionality / Transition metal complexes / Dynamics, intramolecular

The mechanisms of intramolecular dynamics in transition metal hydride complexes are surveyed in this review. The NMR data for a number of fluxional hydrides are interpreted in terms of principal and secondary topological changes of the coordinated ligands. The principal ligand motions can be further categorized as being of migratory (**M**) and replacement (**R**) type. Discussion of these ligand motions is followed by analysis of more complex rearrangements of hydride systems, in which both types are operative in multiple exchange processes. The attempted systematic approach appears to be a useful general mechanistic concept for the understanding of the fluxional behavior of hydride complexes.

Contents

Introduction

Many transition metal hydride complexes are stereochemically nonrigid in solution. As a result, most reviews on hydride chemistry include some discussion of the dynamic behavior of such molecules[1]. Systematic spectroscopic studies of the fluxionality of hydrides were started in the early 70's, to a great part by the efforts of Meakin, Muetterties and co-workers[2]. These investigations included five-, six-, and eight-coordinate complexes: MHL_4[2e], MH_2L_4[2a,b,d,f], MH_4L_4[2c,g] (e.g., M = Mo, W, Os, Ru, Fe, Co, Rh, Ir and L = phosphorus ligands). All classes of coordination compounds examined in the H_nML_4 series were stereochemically nonrigid. Low barriers were found in those cases where n = 1 or 2, which were explained on the basis of a tetrahedral jump mechanism. The fluxionality is facilitated as the ML_4 substructure approaches that of a regular tetrahedron. Plausible physical rearrangement mechanisms were suggested for the dodecahedral eight-coordinate MH_4L_4 complexes.

Heinz Berke (right) was born in Bayreuth (Germany) in 1946 and received his Ph. D. from the University of Tübingen in 1974 under the supervision of Prof. E. Lindner. He then joined the University of Konstanz and in 1977 he went for a postdoctoral stay at Cornell University, Ithaca, USA, to work with Prof. R. Hoffmann. After that he continued his research in Konstanz, where he completed his Habilitation in 1981. In 1988 he became full professor at the University of Zürich. His research concerns transition metal organometallic chemistry with emphasis on hydride and cumulenylidene complexes and the development of reactive metal centers.

Dmitry G. Gusev (left) was born in Petropavlovsk (Kazakhstan, USSR) in 1960. He graduated from the Moscow Institute of Fine Chemical Technology and received there his kandidat (Ph. D.) degree in 1986. Afterwards he joined the NMR laboratory of the Institute of Organo-Element Compounds in Moscow. Since 1992 he has been a research associate working with Professors Kenneth G. Caulton at Indiana University, Bloomington, USA, and Heinz Berke at the University of Zürich.

  0009–2940/96/1010–1143 $ 15.00+.25/0

Further progress in hydride chemistry then became possible, when many more new examples of hydride fluxionality were discovered. The investigations of these were predominantly synthetic studies, which only rarely pursued spectroscopic characterization. These reports have often included variable-temperature NMR data for the temperture range 20 to −80 °C, a range that is normally inappropriate to reach limiting slow-exchange NMR spectra. Unfortunately, this happened quite often for those cases that appeared to be highly intriguing from the structural point of view and for which structural elucidation was difficult, for example, the polyhydrides MH_nL_m ($n \geq 3$). Since the time of the early spectroscopic analyses mentioned above, the question of the exchange mechanisms operating in metal hydrides has never been addressed in a systematic fashion, neither experimentally nor theoretically.

For a number of years our research on hydride complexes of Re, Fe, Ru, Os, and Ir has encountered a variety of fluxional systems. In the present report we review the essential features of the observed processes with emphasis on mechanistic interpretations of the dynamic phenomena. Although the discussion will include additional examples from the current literature, this article cannot be considered a comprehensive review. It does not attempt an interpretation of all known fluxional hydrides, but rather concentrates on the principal mechanistic aspects, which will be illustrated with appropriate examples.

1. Principal Exchange Types

Ligand exchange in a metal complex is a process of physical rearrangement (motion) of an ensemble of atoms in the coordination sphere. Let us imagine an observer, who could have labeled the metal-bound atoms in a fluxional complex, to subsequently take several snapshots of the molecule during the rearrangement process. Examining the starting and final topologies of atoms (i.e., ground-state structures) referenced to the coordinate system of the observer, one would find a number of atoms with *unchanged* (or *little changed*) positions, while the others reveal *substantially altered* coordinated. When we refer to the process of the positional changes of the latter atoms, we can denote this the **principal motion.** The term **secondary motion** (secondary rearrangement) can be used to describe those additional structural deformations that occur along with the principal motion. These can be identified by comparison of the ground state and the transition state structures. The secondary topological changes reduce the energy of the transition state and support the principal motion.

In order to ascribe the mechanism for a particular fluxional process, one should try to interpret the experimental dynamic NMR data in the following way: (a) identify those atoms or atomic groups that change their positional coordinates, (b) assign a reasonable pathway for the given principal motions, and (c) evalute what kind of secondary rearrangement might be operative.

Apparent mechanistic principles suggest that in such analyses of dynamic problems one should be looking for least energy pathways for the principal motion conceivable in terms of the particular ligand environment. The exchange barriers are quite often low (10 to 6 kcal/mol and even lower in some cases) in fluxional hydride complexes implying that lighter and smaller atomic groups (ligands) might show a higher probability for "scrambling" or moving, whereas the heavy ligand skeleton would be involved in topological changes of the secondary type.

Apart from the physical exchange there is its projection into spectroscopy, which we denote as the phenomenon of **spectroscopic exchange**. It should be recognized that, for instance, a coalescence of chemical shifts in NMR spectroscopy can be effected by the rearrangement of ligands and atoms other than the resonating nuclei. For example, ^{31}P-NMR exchange can result from hydride fluxionality in the absence of any *physical* permutation between the phosphorus ligands.

Apparently, the finding of an universal rationale for all kinds of intramolecular ligand rearrangements is an impossible task. To provide some guidance, however, we decided to highlight two types of principal motion that are often distinguishable in the dynamic behavior of metal hydrides. We can call them a migratory type (**M**) and a replacement type (**R**). An example of the $Ir(H)_2X(PtBu_2Ph)_2$ dihydrides[3] helps to illustrate the meaning of this classification. These d^6 16-electron molecules have a distorted structure, since the idealized trigonal-bipyramidal geometry possesses a higher energy[3d] (Scheme 1, the two *trans*-phosphane ligands are omitted for clarity).

Scheme 1

Migratory (**M**) type exchange

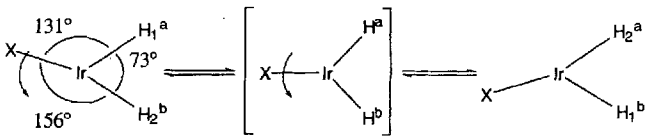

Replacement (**R**) type exchange

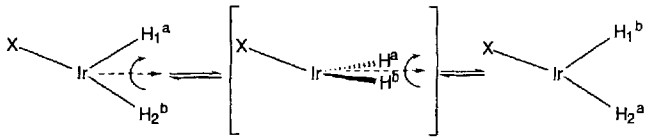

$Ir(H)_2X(P^tBu_2Ph)_2$ (X = Cl, Br, I)

In the **M**-type exchange one or more ligands migrate (move) from the positions that they occupied in the starting ground-state structure. The result of this transformation is an inversion of the whole structure. After this inversion process, those ligands that have migrated do not replace each other in their former coordination sites. In Scheme 1 two protons, labeled H^a and H^b, occupy distinct sites 1 and 2 with different chemical shifts. Mechanism **M** suggests that the 1−2 spectroscopic exchange of the hydrogen atoms proceeds by migration of one ligand X (Scheme 1). In principle the same result can be achieved by another motion, parallel shifts of H^a and H^b in the X, H^a, H^b plane. In the complexes $Ir(H)_2X(PtBu_2Ph)_2$ (X = Cl, Br, I) the exchange rate increases substantially for the lighter halides, indicating that

it is probably migration of the X ligand that determines the kinetics[3f].

The **R**-type exchange is a physical rearrangement of identical atoms or atomic groups (ligands) that exchange their exact positional coordinates. In Scheme 1 hydride H^a replaces H^b, while H^b takes the former position of H^a. Note that in the transition structure H^a and H^b are coplanar with the two phosphane ligands, which implies that the transition distance H···H can be shorter than in the ground state.

Both exchange pathways are thermally accessible in $Ir(H)_2XL_2$ compounds and may have comparable energy barriers. In the actual example of very bulky phosphanes L = P*t*Bu$_2$Ph, the **M** mechanism is probably that of lower energy. The H^a/H^b decoalescence has not been observed for the less bulky P*t*Bu$_2$Me derivative[3f], which might indicate an acceleration of the **R**-type exchange.

Scheme 2

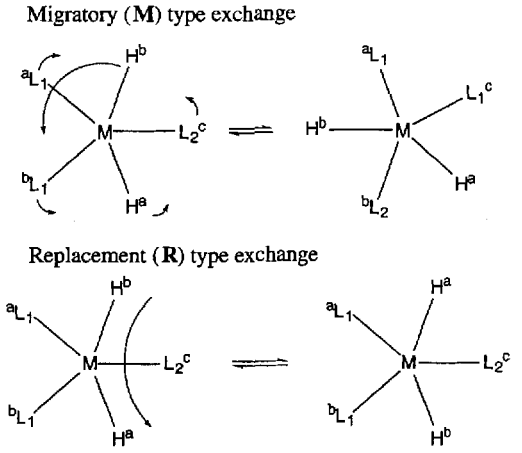

Another example is given in Scheme 2, which shows the equatorial plane of a complex with pentagonal-bipyramidal geometry (actual examples will be discussed in the following three sections). The main features of the rearrangements represented by Scheme 2 are reminiscent of the previous example. In the **R** exchange hydride H^a goes to the site of H^b and vice versa. The other possibility is the **M** process for one hydride, for example, H^b. Only this ligand then moves substantially on its travel from the former site between L^a and L^c to a new site between L^a and L^b. Certain motions of the other ligands, H^a and all L, are required in the equatorial plane. These, however, have the characteristics of secondary motions, in the sense that they assist the migration of H^b.

The examples of Schemes 1 and 2 show that the **M** and **R** mechanisms can be distinguished by NMR if they do not take place simultaneously on the same time scale. The **R**-type process would cause exchange of the chemical shifts of the exchanging ligands and would lead to an averaging of all couplings between these and other magnetic nuclei in the coordination sphere. The important feature of the **M**-type exchange in this system, however, is that this process can result in *spectroscopic exchange* of ligands involved only in secondary topological changes. The principal motion of X in the first example (Scheme 1) leads to exchange of the chemical shifts of H^a and H^b, which does not require any motion of the hydride. Scheme 2 shows how migration of H^b can exchange chemical shifts of L = PR_3 without physical scrambling of these ligands. More examples will be provided in the next three sections.

2. R-Type Exchange

In this chapter a number of fluxional processes is described, which in the essential features display **R**-type characteristics in the dynamic processes.

$M(H_2)L_n$ and $M(H)_2L_n$: Intramolecular twofold reorientation of coordinated dihydrogen is the simplest example of the **R**-type exchange (Scheme 3). The barriers for this fluxional process are often low, 1–3 kcal/mol, as determined by inelastic neutron scattering[4]. In the following discussion it is assumed that two hydrogen atoms at a bonding distance of <1.3 Å always have an easy access to this very efficient scrambling pathway.

Scheme 3

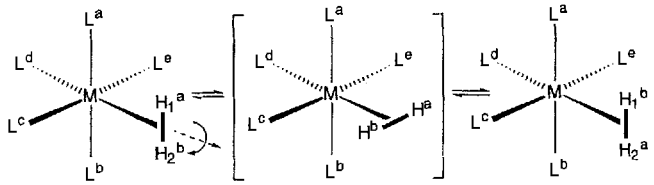

On the other hand, classical dihydrides of octahedral structure $M(H)_2L_4$ with large $H^a\cdots H^b$ separation typically show substantially higher barriers (>10 kcal/mol). For example, the hydride exchange in *cis*-$Re(H)_2(CO)(NO)L_2$ compounds [L = PMe_3, PCy_3, $P(OiPr)_3$] is very slow[5]. In these molecules H^a and H^b are separated by 2.30(5) Å[6], a distance that decreases in the transition state when H^a-H^b eclipses the L–M–L axis[5].

$Os(H)_3X(PiPr_3)_2$: Three trihydrides of osmium (X = Cl, Br, I) have been studied by using NMR[7a] and ab initio calculations[7]. The structure of these d^4 16-electron $Os(H)_3X(PiPr_3)_2$ molecules is C_{2v}-distorted octahedral, with two ligands H^a and H^c exerting a strong mutual *trans* influence and therefore being bent toward H^b (Scheme 4).

Scheme 4

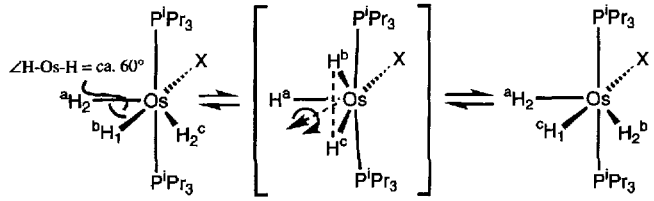

The structural features of $Os(H)_3X(PiPr_3)_2$ are very similar for various halides. Among the spectroscopic properties the most remarkable of these systems is the exchange coupling between the hydrides: they show AB_2 patterns in the ^{1}H-NMR spectrum, with $J(H_1\text{-}H_2)$ values of 920 (Cl), 550 (Br), and 280 Hz (I) at −100 °C. The available observations indicate that exchange coupling can be operative between

hydrogen atoms, if they are involved in the **R**-type exchange[7b,8]. Another example of this behavior is detected in $Os(H)_3(H_2)X(PiPr_3)_2$ complexes, which will be presented below in Section 3.

The rate of the hydride 1–2 site exchange in $Os(H)_3X(PiPr_3)_2$ increases slightly from X = I to X = Cl. The highest barrier was determined experimentally for X = I, $\Delta G^{\neq}$ (205 K) = 8.8 kcal/mol. In ab initio calculations the replacement exchange has been mimicked by an out-of-plane twist of the two adjacent hydrogen atoms, that is H^b and H^c (Scheme 4). Vibrations in this direction are of lower frequency (450 cm^{-1}) compared with the in-plane Os–H bending (900 cm^{-1}). In the optimized transition structure $H^b\cdots H^c$ eclipses the P–Os–P axis, and the H^b–Os–H^c angle decreases to 51.5° (Cl) and 50.4° (I) from that calculated in the ground state: 56.9° (Cl) and 57.5° (I). The $H^b\cdots H^c$ separation thus decreases to 1.38–1.35 Å, which is almost twice the H–H distance in H_2 (0.74 Å) and does not indicate substantial H^b–H^c bonding.

In related fluxional trihydrides $[(C_5H_5)Ir(L)(H)_3]^+$, which also show exchange couplings, calculations suggested the formation of a dihydrogen ligand in the transition structure[8]. That is why the H^b–H^c angle changes from 64.0 to 29.6° (L = PH_3) and from 62.8 to 27.6° (L = CO).

To summarize these results: replacement exchange is a phenomenon of general occurence in complexes with (at least) two *cis*-disposed hydride ligands. It is facilitated when the hydrogen atoms are situated relatively close in the ground state structure. Additional shortening of the H···H distance "on the move" decreases the exchange barrier.

Scheme 5

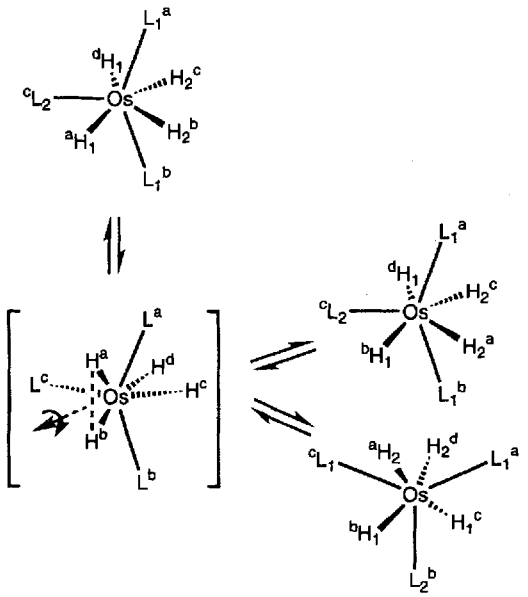

$Os(H)_4L_3$: Osmium tetrahydrides with L = phosphane ligands have a distorted pentagonal-bipyramidal structure as shown in Scheme 5[9]. The molecules are all highly fluxional both in the ^1H- and ^{31}P-NMR spectra. For one case, L = PMe_2Ph, has decoalescence been reported in a [D_8]toluene/CF_2Cl_2 mixture[10]. Two equally intense hydride resonances and ^{31}P resonances of 2:1 intensity were observed at −120 °C. Scheme 5 shows two scenarios explaining the fluxionality. Hydrides H^a and H^b (also H^c and H^d) exchange sites by the 1–2 **R**-type exchange. This exchange is presumably accompanied by a deformation of the OsL_3 fragment in the transition state to form an equilateral L^a–L^b–L^c triangle and subsequent opening of either L^a–Os–L^c or L^b–Os–L^c. By this pathway the phosphorus chemical shifts can also be exchanged.

$[Re(H)_2(CO)(PMe_3)_4]^+$[11a] **and $Re(H)_2(\eta\text{-}C_6H_4\text{-}PPh_2)(PEt_3)_3$**[11b]: These two fluxional ruthenium dihydrides are well-characterized by NMR and X-ray and differ from the previous examples in that the two exchanging hydrides are separated by a third ligand. The essential features of the solid state structures are given in Scheme 6.

Scheme 6

$[Re(H)_2(CO)(PMe_3)_4]^+$ $Re(H)_2(\eta^2\text{-}C_6H_4\text{-}PPh_2)(PEt_3)_3$

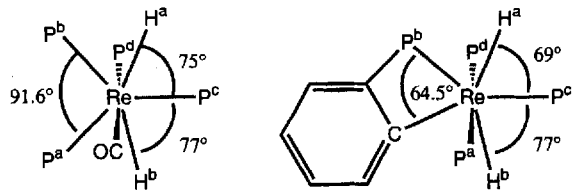

In both molecules all bonds to rhenium are strong, and it has been proven that ligand dissociation does not occur during the exchange of the magnetically nonequivalent hydrogens H^a and H^b. This process apparently involves hydrides and does not bring about any site exchange in the heavy ligand skeleton of $Re(H)_2(\eta^2\text{-}C_6H_4PPh_2)(PEt_3)_3$, because the barrier for the H^a/H^b scarmbling is $\Delta G^{\neq}$ = 12.7 kcal/mol (28 °C), whereas the P^a, P^c, P^d exchange proceeds through a higher energy transition state with $\Delta G^{\neq}$ = 15.1 kcal/mol (38 °C)[11b].

A viable mechanism for the fluxional processes in both molecules is depicted in Scheme 7. It shows how one of the hydrides, e.g. H^a, can migrate through a P–Re–P plane to form an intermediate structure with a *cis*-ReH_2 fragment. When the ground state geometry is restored, H^a and H^b have equal chances to reach either position 1 or remain in 2.

The example of $[Re(H)_2(CO)(PMe_3)_4]^+$ is important because both isomeric forms, the pentagonal-bipyramidal dihydride and the octahedral dihydrogen complexes, have been observed experimentally and characterized by NMR[11a]. The dihydrogen complex is a kinetic product of the protonation of *cis*-$ReH(CO)(PMe_3)_4$. It can be prepared at low temperature, and the isomerization takes place in the temperature range of −20 to 0 °C.

For $Re(H)_2(\eta^2\text{-}C_6H_4\text{-}PPh_2)(PEt_3)_3$ the intermediate of Scheme 7 may possess no H^a–H^b bonding interaction, since this complex is neutral and bears no strong π-acceptor ligand like CO. The cationic and neutral dihydrides differ slightly in that the former apparently has an alternative possibility for hydride migration: either H^a or H^b can migrate

Scheme 7

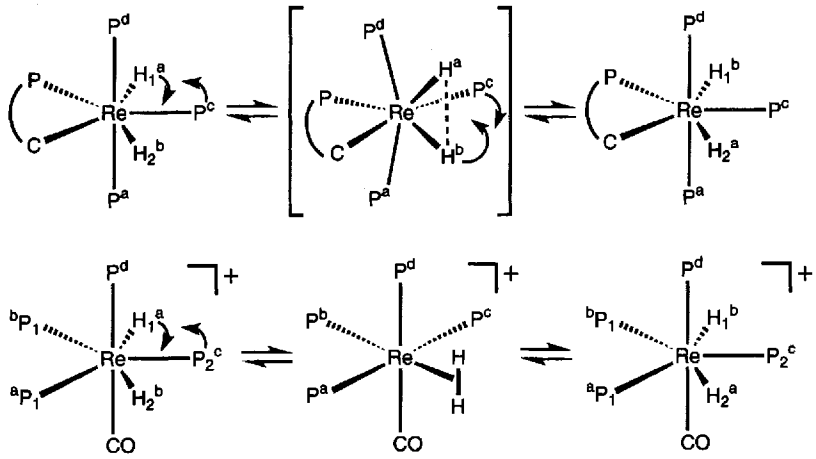

to a position between the P^a and P^b ligands in the equatorial plane. The structure of $[Re(H)_2(CO)(PMe_3)_4]^+$ is then inverted: $\langle P_1^a, P_1^b, P_2^c\rangle$ becomes either $\langle P_2^c, P_1^b, P_1^c\rangle$ or $\langle P_1^a, P_2^b, P_1^c\rangle$. The total fluxional process in Scheme 7 represents replacement of one hydride by another, while the principal motion in the formation of the intermediate is the passage of one hydride between two ligands, which requires opening of the P–Re–P (or P–Re–CO) angle in the transition state. This must be a high-energy process and explains the relatively large barrier of ca. 13 kcal/mol in $Re(H)_2(\eta^2\text{-}C_6H_4PPh_2)(PEt_3)_3$.

3. M-Type Exchange

$Os(H)_2XYL_2$: The type of complex to be discussed first belongs to another family of distorted d^4 16-e complexes. The solid-state structure with identical halides X = Y = Cl and L = $PiPr_3$ revealed perpendicular H^a–Os–H^b and L–Os–L planes[12a]. The Cl–Os–Cl fragment is twisted by ca. 45° with respect to the former two. This structure makes H^a and H^b inequivalent when X ≠ Y, and the complexes $Os(H)_2ClBr(PiPr_3)_2$, $Os(H)_2ClI(PiPr_3)_2$, and $Os(H)_2BrI(PiPr_3)_2$ exhibit intrinsic H^a/H^b decoalescence in the ^{1}H-NMR spectra, which is not observed for X = Y[12b].

Scheme 8 shows some structural features of $Os(H)_2XYL_2$ together with a suggested mechanism supporting the *spectroscopic* hydride exchange, which assumes simultaneous migration of the two ligands X and Y. The fluxionality is substantially influenced by the nature of X and Y and becomes more facile in the following order: XY = BrI < ClI < ClBr. The Arrhenius activation energy is the same for $Os(H)_2ClI(PiPr_3)_2$ and $Os(H)_2BrI(PiPr_3)_2$ (E_a = 9.4 and 9.6 kcal/mol, respectively) which is determined by the nature of the barrier. The pre-exponential factor is, however, larger for the former complex ($19.5 \cdot 10^{-12}$ vs. $0.9 \cdot 10^{-12}$ s^{-1}), which reflects a higher frequency of attempts to overcome the barrier for the lighter halide.

Ab initio calculations[12b] have revealed that the transition structure in Scheme 8 with P···P eclipsing X···Y is actually a ground state structure of $Os(H)_2Cl_2(PH_3)_2$. The

Scheme 8

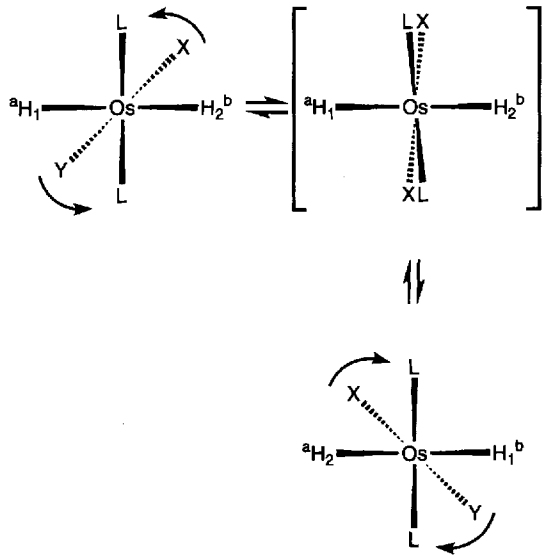

distorted experimental geometry of $Os(H)_2Cl_2(PiPr_3)_2$ is presumably dominated by repulsions between the halides and the bulky phosphane ligands. The **R**-type exchange of H^a and H^b between sites 1 and 2 is not accessible because of the small $PiPr_3$–Os–$PiPr_3$ bite angle (112°)[12a].

$M(H_2)(H)_2XL_2$: These complexes have a pseudo-octahedral structure with a dihydrogen ligand *trans* to a hydride (Scheme 9)[4b,13e,f]. All representatives of the $M(H_2)(H)_2XL_2$ series are highly fluxional[3a,c,13]. For the case of $Ru(H_2)(H)_2(CO)(PiPr_3)_2$ the barrier was ca. 8 kcal/mol and three ^{1}H resonances of H^a, H^b, and H* were observed in the hydride region below −100 °C[13e].

The solid-state ^{1}H-NMR spectrum of a single crystal of $Ir(H_2)(H)_2Cl(PiPr_3)_2$ provided the key information on the fluxional behavior of this molecule[14]. A transition state of C_{2v} symmetry is achieved by stretching the H–H bond and

Scheme 9

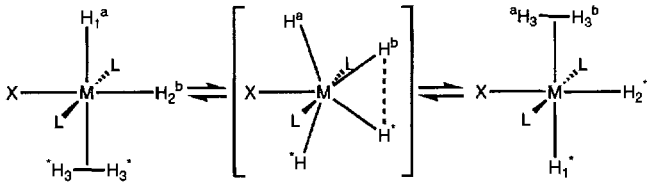

$M(H_2)(H)_2L_3$ (M = Fe, Ru)
$M(H_2)(H)_2(CO)L_2$ (M = Ru, Os)
$Ir(H_2)(H)_2XL_2$ (X = Cl, Br, I)

by subsequent concerted movement (migration) of the metal-bound hydrogen atoms. This transient structure can be inverted in a fashion shown in Scheme 9 with the hydrogen atoms H^a and H^b forming a new H_2 ligand. All this happens in the equatorial plane of the molecule. The NMR results are not consistent with H^b-H^* rotation, i.e., they suggest no hydrogen ligand transfer between the two sides of the X–M–L plane. H^a/H^b site exchange is accomplished by facile H_2 spinning.

For different $M(H_2)(H)_2XL_2$ species the $H^b\cdots H^*$ separation in the transition structure is expected to depend on X. The π acceptor CO favors formation of an H_2 ligand in the *trans* position. This idea has been substantiated further by ab initio DFT calculations on $M(H)_2(H_2)(CO)(PH_3)_2$ (M = Ru, Os), in which the H^b-H^* distance became as short as 0.844 and 0.894 Å, and the transition state structures were 7.9 and 6.1 kcal/mol, respectively, above the ground state[13f]. The calculated energy for M = Ru was in excellent agreement with the experimental barrier of ca. 8 kcal/mol[1f,13e].

The π-donation property when X = halide is expected to favor the rupture of a *trans* H_2 ligand[15]. The *trans* structure of $Ir(H_2)X(H)_2L_2$ may have a relatively large $H^b\cdots H^*$ separation, which presumably explains why H^b and H* do not rotate on the time scale of the migrational exchange in this molecule.

$[M(H)_3L_4]^+$: Recently we have prepared and characterized several trihydrides $[M(H)_3L_4]^+$ [L = PMe_3 (M = Fe, Os); L = PEt_3 (M = Fe, Ru, Os)]. The solid-state structures of $[Fe(H)_3(PEt_3)_4]^+$[16] and of the related $[Os(H)_3(PPh_3)_4]^+$[17] show an approximate tetrahedral ML_4 skeleton, which is capped by hydrides on three of the four faces.

A fluxional process averaging the AA′A″XX′X″Y (A = ^1H; X = Y = ^{31}P) spin system has been interpreted[16,17] in terms of the "tetrahedral jump" mechanism[2], which assumes migration of one hydride ligand from an occupied face onto an empty one (Scheme 10). The chemical shifts of the shaded phosphorus nuclei are exchanged by this hydride motion.

Scheme 10

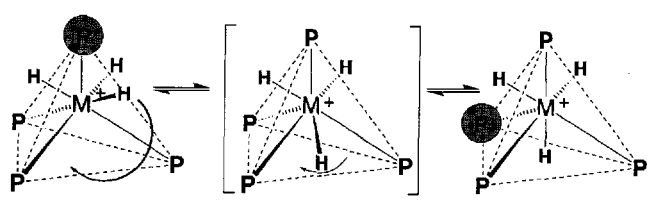

Scheme 11 suggests another view of the transition state than that depicted in Scheme 10. The first and second structures on the left represent two views of the principal motion in the transition state geometry in which hydrides H^a and H^b and four phosphorus ligands still occupy their ground state positions. The third hydride is on the move and has already reached the plane of the four ligands H^a, H^b, P^a, and P^b. The second structure in Scheme 11 then additionally indicates the obvious directions in which the secondary ligand rearrangement would preferably occur. This is opening of the P^a-M-P^b angle in the newly formed pentagonal plane followed by a concomitant closing movement of the hydrides H^a and H^b. In addition, the P^c-M-P^d angle is expected to increase, which would bring the two phosphanes close to the axial positions. The structure on the right is a "refined" model for the transition state.

It is remarkable that the shape of this molecule has now closely approached that of the two complexes of pentagonal-bipyramidal geometry, $Re(H)_3(PPh_2Me)_4$[18] and $Re(H)_3(CO)(PMe_3)_3$[11a], characterized by X-ray analysis. In the solid-state structure of $[Fe(H)_3(PEt_3)_4]^+$ the P^a-Fe-P^b angle is 102°, which will be enlarged to 136–137° in the transition structure (Scheme 11). This is ca. 17° for the bending of each M–P bond. Another angle between phosphorus ligands, P^c-Fe-P^d, is 122°, which will probably open to 160°. This amounts to ca. 19° for the M–P bending. The transition-state $H^b\cdots H^a$ distance should vary greatly with M and PR_3. In the Fe–Ru–Os triad a distorted octahedron with close H^b-H^a contact in the *trans* position to H^c is unknown in complexes with monodentate phosphanes. In all cases of M and PR_3 such a geometry is presumably at higher energy than the possible alternative structures. The same conclusions have been drawn from DFT calculations on $[FeH_3(PMe_3)_4]^+$ complexes[19].

When the passage of H^c through P^a and P^b is complete, the heavy-ligand skeleton relaxes back to the former geometry with only small changes of the positional coordinates. P^c and P^d are interconverted with respect to H^c. For instance, the $M-P^c$ bond length, which is longer (since *trans* to the hydride) than that of $M-P^d$ before the H^c jump, becomes the shortest after this migration. The heavy-ligand motion can be visualized as "breathing" and would belong to the secondary type motion.

The barrier for the jump is determined by a combination of steric and electronic factors and increases in the order: $PMe_3 < PEt_3 < PPh_3$, because of the increasing repulsion experienced by a hydride between two phosphanes. We have also observed that the fluxionality becomes easier in the order Fe < Ru < Os, for example, $\Delta H^{\neq}$ = 10 (Fe) > 7.4 (Ru) > 6.4 kcal/mol (Os) in $[M(H)_3(PEt_3)_4]^+$[16]. This second trend should be determined by the relative stability of the two isomeric forms of $[MH_3(PR_3)_4]^+$, which are shown as the ground and transition state species in Schemes 10 and 11. Apparently, the energy difference becomes smaller down the triad, although it is not amenable to any qualitative evaluation. Another series of molecules with nearly

Scheme 11

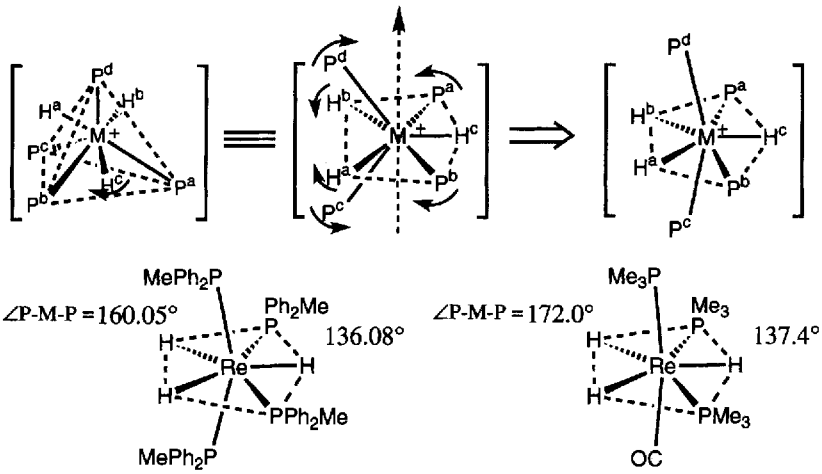

tetrahedral heavy-ligand skeletons, anionic $[MH(PF_3)_4]^-$ (M = Fe, Ru, Os) and neutral $MH(PF_3)_4$ (M = Co, Rh, Ir) complexes, show the opposite trend $\Delta H^{\neq} = < 5$ (Fe) < 7 (Ru) < 8 kcal/mol (Os), $\Delta H^{\neq} = 5.5$ (Co) < 9 (Rh) < 10 kcal/mol (Ir)[2e]. This could mean that a different mechanism of fluxionality is operative in these cases (i.e., Berry pseudorotation), but not necessarily, since the tetrahedral jump represents a very plausible alternative from the point of view of "least motion".

Scheme 12

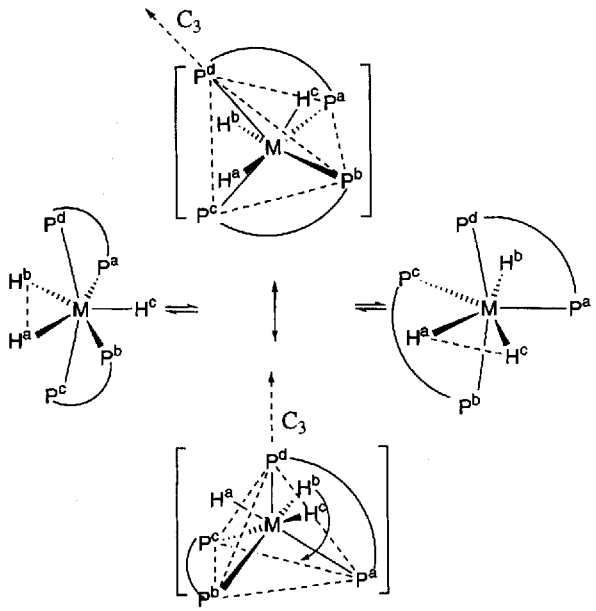

Rearrangements shown in Schemes 10 and 11 provide an explanation for the dynamic behavior of the other complexes with seven metal-bound atoms, in which the ground state structure is either pentagonal-bipyramidal[11a,18,20], as in $Re(H)_3L_4$, or distorted octahedral[1h,21], as in $[MH(H_2)L_4]^+$ (M = Fe, Ru, Os). The situation is now inverted in the sense that the ground state structure (Scheme 12) has the shape of the transition geometry in Scheme 11. However, on the transformation path the ligand ensemble carries out the same movements, i.e., the breathing motion of the heavy-ligand skeleton is expected to eventually make the hydrides H^a, H^b, and H^c equivalent around the pseudo-C_3 symmetry axis.

This explanation is fully consistent with the experimental observation of an acceleration of the intramolecular hydrogen exchange when the size and flexibility of the diphosphane (P^a-P^d and P^b-P^c) chelate rings increase. For example, $[RuH(H_2)(dppb)_2]^+$ [dppb = 1,2-bis(diphenylphosphanyl)butane] is more fluxional than $[RuH(H_2)(dppp)_2]^+$ [dppp = 1,2-bis(diphenylphosphanyl)propane], which is, in turn, more fluxional than $[RuH(H_2)(dppe)_2]^+$ [dppe = 1,2-bis(diphenylphosphanyl)ethane][22a]. The same is true for rhenium trihydrides, in which, for instance, hydride exchange in $Re(H)_3(dppe)(PPh_3)_2$ is much faster than in $Re(H)_3(dppe)_2$[22b].

In an early publication, in which an attempt was made to interpret the fluxional behavior of the rhenium complexes, a tricapped tetrahedral intermediate was considered unlikely because of "the relatively large heavy atom motions required to reach it"[22b]. One could argue that bending of the M–P bonds by 17–19° (Schemes 11, 12) may actually be envisaged as a process of relatively low-energy deformations. Bulky chelating ligands P–P = dppf [1,2-bis(diphenylphosphanyl)ferrocene] and dcpe [1,2-bis(dicyclohexylphosphanyl)ethane] are known to favor the tetrahedral structure as a ground state[23]. Note, however, that the *trans*-$OsH(H_2)Cl(CO)L_2$ complexes (L = P*i*Pr$_3$, P*t*Bu$_2$Me) are quite rigid at room temperature[24]. These molecules have a strong preference for a planar $OsCl(CO)L_2$ arrangement with two *trans*-disposed bulky phosphanes and also the π donor Cl *trans* to the π acceptor CO. Apparently a low-energy tetrahedral deformation is not available in this substructure. The H/H_2 scrambling can presumably take place only if a hydrogen released from the H_2 ligand can manage to squeeze through the $OsCl(CO)L_2$ plane.

4. Complex Exchanges

In this section we will consider examples of rhenium and osmium polyhydrides which show a plethora of dy-

namic features as a combination of **M** and **R** exchange types.

$[Re(H)_4(CO)L_3]^+$ and $[Re(H_2)(H)_2(CO)L_3]^+$: The MH_4L_4 structural type is a remarkably rich case. For instance, the $[ReH_4(CO)L_3]^+$ complexes (L = PMe_3, PMe_2Ph) exist in solution as two isomers in equilibrium, and both show facile hydride fluxionality. The PMe_2Ph complex was discovered by Luo and Crabtree[25a,b] and, after shortly we encountered the PMe_3 analogue in our research[11a].

Figure 1. Low-temperature ^1H-NMR spectra (CD_2Cl_2, 300 and 500 MHz) of the two isomers of $[ReH_4(CO)(PMe_3)_3]^+$[11a] and the D isotopomers $[Re(H,D)_4(CO)(PMe_2Ph)_3]^+$[25a,b] and $[Re(H,D)_4(CO)(PMe_3)_3]^+$[11a] in the hydride chemical shift region

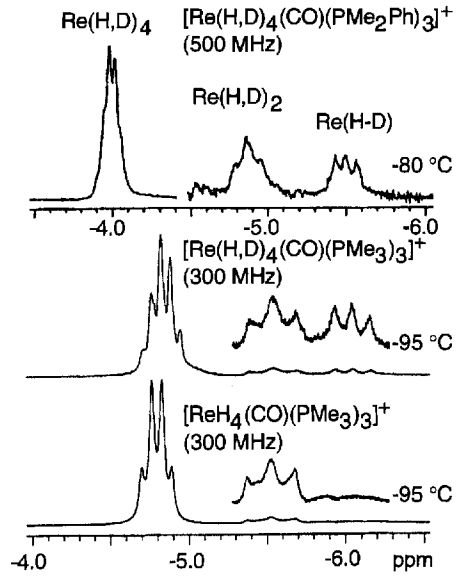

Both molecular systems are almost identical in the low-temperture ^1H-NMR spectra (Figure 1), where the tetrahydrides $[Re(H)_4(CO)L_3]^+$ show one exchange-averaged quartet in the hydride region, while decoalesced $Re(H_2)$ and $Re(H)_2$ resonances are seen for the dihydrogen isomers $[Re(H_2)(H)_2(CO)L_3]^+$.

The case L = PMe_2Ph has not been characterized by variable-temperature ^{31}P NMR. The $^{31}P\{^1H\}$-NMR spectra of $[ReH_4(CO)(PMe_3)_3]^+$ are presented in Figure 2 and show that the heavy-ligand skeleton is quite rigid in the tetrahydride, while surprisingly fluxional in the dihydrogen complex. This observation contrasts the dynamic behavior in the ^1H-NMR spectra.

Solid-state (X-ray) structural data are not available for the $[ReH_4(CO)L_3]^+$ cations because of the thermal instability of these molecules, which decompose in solution above −40 °C. A dodecahedral structure (Scheme 13) has been suggested for the tetrahydride isomer in both cases, L = PMe_3 and PMe_2Ph. For $[Re(H)_4(CO)(PMe_3)_3]^+$ this is supported by the observation of a doublet of triplets in the $^{13}C\{^1H\}$-NMR resonance of the CO ligand, with a *trans* ^2J(C-P) = 24.1 Hz and a small *cis* ^2J(C-P) = 5.6 Hz coupling[11a]. This tetrahydride retains many structural features of the neutral precursor $Re(H)_3(CO)(PMe_3)_3$ (Scheme 11), which also shows a doublet of triplets (±51.0/∓ 11.7 Hz) CO resonance[11a]. A dodecahedral structure has been established for a related $[Re(H)_4(PMe_2Ph)_4]^+$ complex by X-ray crystallography[26].

Figure 2. Variable-temperature $^{31}P\{^1H\}$-NMR (CD_2Cl_2, 121.4 MHz) spectra of two isomers of $[ReH_4(CO)(PMe_3)_3]^+$[11a]. A decomposition product, which appears at −40 °C, is marked by an asterisk

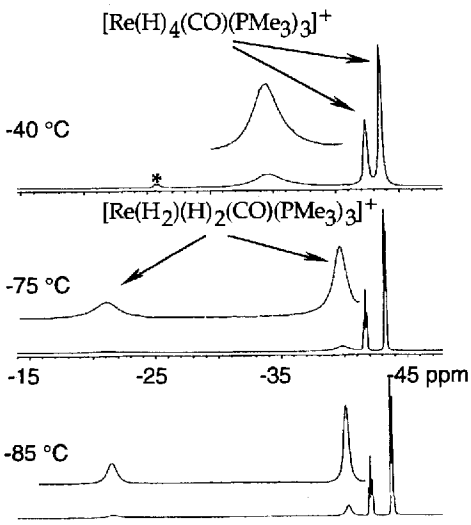

Two mechanisms suggested in Scheme 13 involve two possible deformations of the $Re(CO)L_3$ skeleton: flattening motion (A) and deformation (B) toward a tetrahedral arrangement. Pathway A provides conditions for a fast pairwise hydride migration and their eventual replacement exchange. The transition state structure in B possesses a C_3 symmetry axis through CO-Re-H^c; one of the ligands L^a, L^b, L^c occupies the apical position (pseudo-*trans* to CO) on completion of the rearrangement. Mechanism A is in agreement with the experimental observation (Figure 2) that ^{31}P exchange does not occur on the time scale of hydride exchange.

Scheme 13

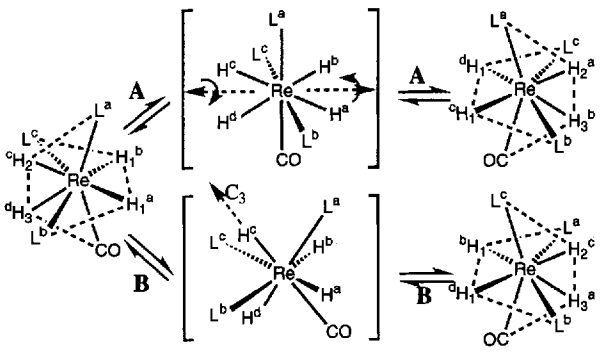

The dodecahedral geometry quite often represents a deep minimum on the potential energy surface of eight-coordination. Rearrangement barriers are typically high (12.5−15 kcal/mol), for example for the tetrahydrides $M(H)_4L_4$ (M =

Mo or W, with L = phosphorus ligands), and these molecules therefore appear to be relatively rigid[2g]. The fluxionality exhibited by $[Re(H)_4(CO)L_3]^+$ is rather an exception to the general behavior.

The structure and dynamics of the nonclassical isomer $[Re(H_2)(H)_2(CO)L_3]^+$ are more intriguing. There is a certain disagreement in the literature[11a,25a,b,27] on the structural interpretation of the NMR data for $[Re(H_2)(H)_2(CO)(PMe_2Ph)_3]^+$ and $[Re(H_2)(H)_2(CO)(PMe_3)_3]^+$. Figure 3 shows a hydride-coupled ^{31}P-NMR spectrum of the latter complex at −110 °C, which displays an AA'XX'Y spin system (neglecting very small couplings between the phosphorus nuclei and the proton atoms of the coordinated H_2) which means that from the angles around the Re center ∢A−Re−X = ∢ A'−Re−X' and ∢A−Re−X' = ∢A'−Re−X. The seven-coordinate molecules $[Re(H_2)(H)_2(CO)L_3]^+$ thus have four nuclei of A, A' = ^1H and X, X' = ^{31}P in one plane. In addition, there must also be a molecular symmetry plane containing Re, CO, H_2 and one L ligand, which bisects the former.

Figure 3. Experimental (bottom) and simulated (top) hydride-coupled ^{31}P-NMR (121.4 MHz) spectra of $[Re(H_2)(H)_2(CO)(PMe_3)_3]^+$ under slow-exchange conditions (−110 °C) in CD_2Cl_2/[D_8]toluene (5%). AA'XX'Y (A = ^1H, X = Y = ^{31}P) spin system. ^2J(X-Y) = 26, ^2J(A-Y) = 44, ^2J(A-X) = 47, ^2J(A-X') = ca. 1 Hz

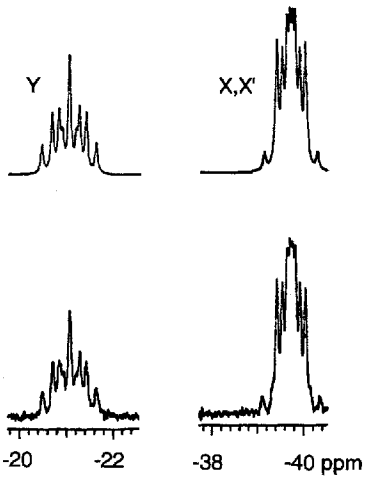

All requirements would be satisfied by two different pentagonal-bipyramidal geometries suggested in the literature for $[Re(H_2)(H)_2(CO)(PMe_2Ph)_3]^+$ and $[Re(H_2)(H)_2(CO)(PMe_3)_3]^+$. Only one of these structures (Scheme 14), however, is correct: the ^1H-NMR spectra in Figure 1 leave no doubt that both L = PMe_2Ph and PMe_3 molecules have the same structure.

The observation of a quartet ^{13}CO resonance [^2J(C-P) = 9 Hz] in $[Re(H_2)(H)_2(CO)(PMe_3)_3]^+$ at −95 °C would support the view that all PMe_3 moieties are in one plane in the ground state molecules. Additional insight is provided by an analysis of the fluxional behavior. The most crucial piece of dynamic information is that the $^{31}P\{^1H\}$-NMR spectra (Figure 2) reveal a remarkably fast exchange in the dihydrogen complex.

Scheme 14

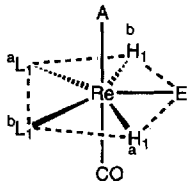

$[Re(H_2)(H)_2(CO)(PMe_3)_3]^+$:
axial ligand A = H_2, equatorial ligand E = PMe_3
$[Re(H_2)(H)_2(CO)(PMe_2Ph)_3]^+$:
axial ligand A = PMe_2Ph, equatorial ligand E = H_2

The kinetic data obtained by simulation of the variable-temperature spectra of $[Re(H_2)(H)_2(CO)(PMe_3)_3]^+$ have established[11a] that the exchange rates and barrier heights are essentially identical in the ^1H- and ^{31}P-NMR spectra: $\Delta G^{\neq}$ (185 K) = 8.6 (^1H) − 8.7 (^{31}P) kcal/mol, the rates at this temperature are 230−240 s^{-1} (^1H) and 226 s^{-1} (^{31}P); activation parameters from the ^{31}P-NMR spectra: $\Delta H^{\neq}$ = 8.0(2) kcal/mol and $\Delta S^{\neq} = -3.7(1.0)$ eu. The kinetic analysis also reveals an isotope effect k_H/k_D = 2 at 183 K [$\Delta H^{\neq}$ = 8.6(2) kcal/mol and $\Delta S^{\neq} = -1.7(1.0)$ eu] in the deuterated $[ReH_nD_{4-n}(CO)(PMe_3)_3]^+$ species (determined by ^{31}P NMR). It appears that $(H_2)/(H)_2$ scrambling in $[Re(H_2)(H)_2(CO)L_3]^+$ could be responsible for the *spectroscopic* exchange observed by ^{31}P NMR. The structure of the $[Re(H_2)(H)_2(CO)L_3]^+$ compounds should enable us to provide a reasonable pathway for such a motion, which is expected to be of the **M** type.

The structure suggested in Scheme 14 for $[Re(H_2)(H_2)(CO)(PMe_2Ph)_3]^+$ does explain the ease of the $(H_2)/(H)_2$ scrambling (see a related example in Scheme 9 with exchanged energies of the ground and transition states). There would not, however, be any apparent reason for any fast ^{31}P exchange. This seven-coordinate geometry shows only slow ^{31}P exchange in the case of a similar $[Re(H)_2(CO)(PMe_3)_4]^+$ molecule (Scheme 6). Motions like the trigonal twist of three ligands L = PMe_3 are unlikely to contribute below −50 °C.

In the structure suggested for $[Re(H_2)(H)_2(CO)(PMe_3)_3]^+$ the H_2 ligand could interact in an attractive fashion (hydrogen bonding type) with one of the neighboring hydrides, for example, with H^b (Scheme 15). This weak bonding has been well-recognized in crystallographic and theoretical studies and is thought to be responsible for the very fast H/H_2 scrambling in *cis*-$MH(H_2)L_n$ dihydrogen complexes[28]. In the transition state (Scheme 15) the $H^b\cdots H^c$ and $H^c\cdots H^d$ separations are equal; similarly, the angles L^a-Re-L^b and L^a-Re-L^c have the same size. When the rearrangement is complete, the structure has been inverted. The principal motion represents a concerted migration of the H^b, H^c, and H^d hydrogen atoms, which effects the spectroscopic exchange of the phosphorus chemical shifts without physical exchange between these ligands.

Scheme 15

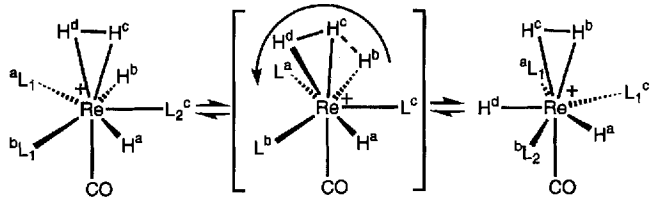

Finally, the mechanism of isomerization between $[Re(H)_4(CO)L_3]^+$ and $[Re(H_2)(H)_2(CO)L_3]^+$ will be explained on the basis of Scheme 16. The ligand scrambling could take place by a clockwise rotation of the $CO-H^d-H^c-L^c$ trapezoid. The transition state structure retains the features of a dodecahedron, which should be of relatively high energy, since all bulky ligands L are in the A sites. When the rotation is complete, two hydrogen atoms H^d and H^c prefer η^2-H_2 coordination. The dihydrogen ligand is supposedly not stretched, because of poor back-donation expected for a coordination site *trans* to a strong π acceptor ligand like CO. The isomerization is quite a slow process (^{31}P line coalescence should be well above $-40\,°C$ for L = PMe_3, Figure 2). The barrier $\Delta G^{\neq}$ was determined for L = PMe_2Ph to be between 12.6 and 11.6 ($\pm$ 0.4) kcal/mol (278 – 213 K)[25b].

Scheme 16

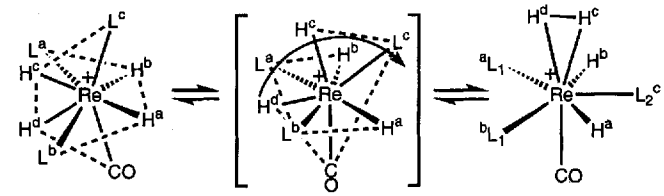

$Re(H)_5L_3$, $[Os(H)_5(PMe_2Ph)_3]^+$, and $Os(H_2)(H)_3X(PiPr_3)_2$: The structure of these complexes with five metal-bound hydrogen atoms is shown in Scheme 17. All rhenium molecules and $[Os(H)_5(PMe_2Ph)_3]^+$ are pentahydrides with a distorted dodecahedral geometry. The structure of $Os(H_2)(H)_3X(PiPr_3)_2$ (X = Cl, Br, I) should be described as a pentagonal bipyramid with H_1-H_2 coordinated in η^2-H_2 fashion[7a,29a,b]. Scheme 17 shows a numbering scheme of the hydrogen atoms together with the most important structural parameters taken from the neutron diffraction studies on $Re(H)_5(PMePh_2)_3$[30] and $[Os(H)_5(PMe_2Ph)_3]^+$[31].

The dodecahedral geometry in $Re(H)_5(PMePh_2)_3$ consists of two trapezoidal planes. One of these, $P-H_5-H_4-H_3$, is an equatorial plane that is also an approximate mirror plane of symmetry in the coordination sphere. This plane is orthogonal to the other trapezoid $P-H_1-H_2-P$. The equatorial plane, including the $Re-H_{1,2}$ vector, shows angles similar to those in a regular pentagonal bipyramid (72°). The structure of $[Os(H)_5(PMe_2Ph)_3]^+$ is slightly different in that the two hydrogen atoms H_4 and H_5 are shifted toward H_3, and the H_3-Os-H_4 angle is decreased by 13.4°.

Scheme 17

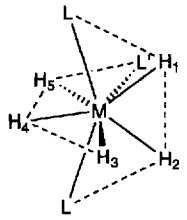

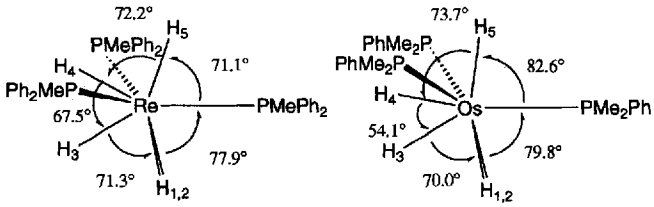

The H_1-H_2 distance is stretched in the dihydrogen osmium complexes $Os(H_2)(H)_3X(PiPr_3)_2$ from 0.95 (X = Cl) to 1.13 Å (X = I), estimated by NMR[29b]. The ab initio DFT calculations established this distance at 0.84 Å in $Os(H_2)(H)_3Cl(PH_3)_2$[29b]. The other structural features of $Os(H_2)(H)_3Cl(PH_3)_2$ are reminiscent of those of $[Os(H)_5(PMe_2Ph)_3]^+$ ($\sphericalangle H_5-Os-Cl$ = 82.8°, $\sphericalangle H_4-Os-H_5$ = 64.4°, $\sphericalangle H_3-Os-H_4$ = 55.5°), except that the two phosphorus ligands are almost *trans* in $Os(H_2)(H)_3Cl(PH_3)_2$.

Slow-exchange ^{1}H-NMR spectra have been reported for $Re(H)_5(AsEtPh_2)_3$[32a], $Re(H)_5(PPh_3)_3$[32b], $Re(H)_5(NC_5H_5)(PPh_3)_2$[32c], and $Os(H_2)(H)_3Cl(PiPr_3)_2$[7a]. Figure 4 shows hydride chemical shifts observed in the rhenium pentahydrides at low temperature. Despite some dependence of these on the nature of the heavy ligands, the general pattern is similar for all complexes and consistent with the solid-state geometry. The coalescence behavior (at elevated temperature) has revealed additional common features.

$Re(H)_5(AsEtPh_2)_3$ is the most instructive example. Figure 5 demonstrates that three independent exchange processes can be distinguished, which average the chemical shifts in this molecule between -135 and $35\,°C$[32a]. The first and slowest (rate constant k_1), responsible for an exchange between the $\langle H_1, H_2, H_3\rangle$ and $\langle H_4, H_5\rangle$ substructures, is frozen out at $-60\,°C$. At this temperature a characteristic 2:3 pattern is observed, which has also been seen at $-60\,°C$ in a related $Re(H)_5(PMe_2Ph)_3$ molecule[30]. $Re(H)_5(PMe_2Ph)_3$ is then rigid on the ^{31}P-NMR time scale (AB_2 pattern) indicating that the hydride fluxionality does not involve any exchange in the ReP_3 skeleton below $-60\,°C$.

The second fluxional process (rate k_2) is the H_4/H_5 site exchange, which becomes slow at $-90\,°C$ producing a 1:1:3 pattern in the hydride region (Figure 5). The process in the related example of $Re(H)_5(NC_5H_5)(PPh_3)_2$ is slower and shows the 1:1:3 hydride spectrum at $-20\,°C$[32c]. Finally, the $\langle H_1, H_2, H_3\rangle$ subspectrum decoalesces below $-120\,°C$ (rate k_3) in $Re(H)_5(AsEtPh_2)_3$ and at $-40\,°C$ in

Figure 4. Schematic representation of the low-temperature slow-exchange ^{1}H-NMR data of three rhenium pentahydrides $Re(H)_5L'L_2$

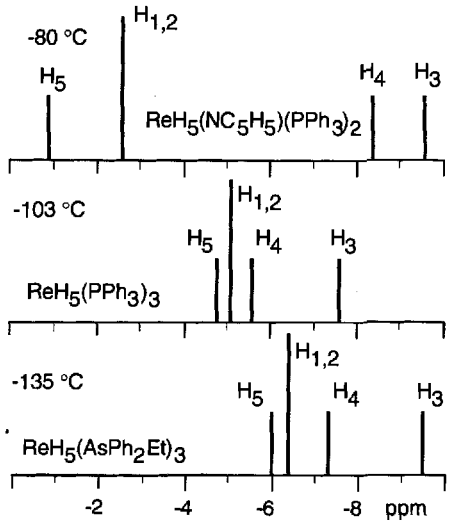

Figure 5. Schematic representation of the variable-temperature data of $Re(H)_5(AsEtPh_2)_3$ showing the ^{1}H-NMR decoalescence behavior ([D$_8$]toluene/$CHFCl_2$)

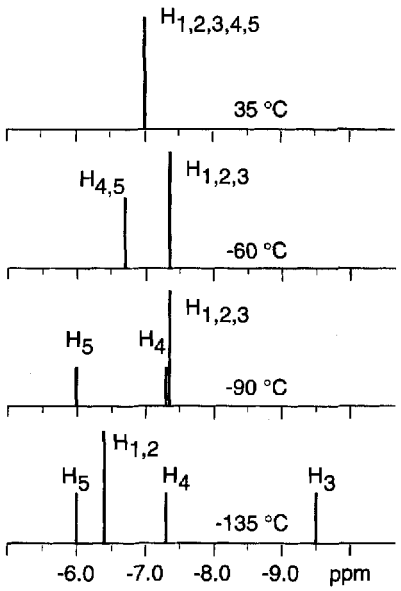

$Re(H)_5(NC_5H_5)(PPh_3)_2$ to display all four inequivalent types of metal-bound hydrogen atoms.

The spectroscopic properties and the fluxional behavior of $Os(H_2)(H)_3X(PiPr_3)_2$ (X = I, Figure 6) show some special features. The first, rather unusual, is the observation of exchange coupling $J(H_3\text{-}H_4)$ = 605 Hz (−128 °C), which increases for lighter halides and reaches ca. 15000 Hz for X = Cl[29a,b]. The chemical shifts of $Os(H_2)(H)_3I(PiPr_3)_2$ are altered with respect to the order given in Figure 4: $\delta H_4 |< \delta H_3$ and $\delta H_5 < \delta H_{1,2}$. The assignment of H_3, although not unambiguous, has been dictated by the observation in the rhenium complex series that H_3 must be that of the neighboring hydrogens $H_{3,4}$, which participate in the fastest exchange of $H_3/H_{1,2}$. It is clear that H_4 and H_3 in Figure 6 are neighbors, since they are exchange-coupled. They are also noticeably shifted to high field (compared with $\delta H_{3,4}$ in the rhenium complexes), which is typical of hydrides *trans* (or pseudo-*trans*) to halide ligands[3f].

It is difficult to establish the actual number of exchange processes operating in $Os(H_2)(H)_3I(PiPr_3)_2$. The appearance of a poorly resolved quartet resonance of H_4 at −104 °C suggests that this is due to the H_4-H_3 coupling averaged by the fastest (rate k_3) exchange of $H_3/H_{1,2}$. The fluxional process involving H_5 (H_4/H_5 scrambling for the rhenium complexes) then proceeds at rate k_2 ($k_2 < k_3$). The observation of a 4:1 intensity ratio at −104 °C is confusing, although this may result from eventual overlap of two broad 1:3 lines of H_5 and $H_{1,2,3}$ in the region between δ = −5 and −7. A third rate constant k_1 is required for the permutation of the H_3 and H_4 sites. The quantum mechanical exchange (exchange coupling) of H_3-H_4 can only occur if there is an H_3/H_4 replacement process.

Figure 6. Variable-temperature ^{1}H-NMR (300 MHz) spectra of $Os(H_2)(H)_3I(PiPr_3)_2$ in $CDFCl_2/CDF_2Cl$[29a,b]

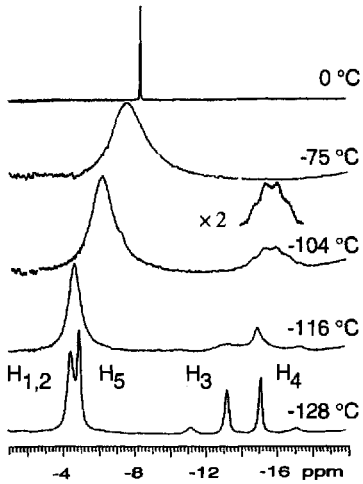

Four mechanisms are therefore suggested and discussed for the processes represented by the rate constants k_1-k_3 in Scheme 18. An additional mechanistic possibility is proposed for the phosphorus ligand exchange. The structures given in brackets represent either transient species or intermediates.

The first process, which accelerates on increasing the temperature (k_3), is considered to be an **R** exchange involving H^a, H^b, and H^c hydrogen atoms. It has been named "turnstile rotation" for $Re(H)_5(NC_5H_5)(PPh_3)_2$, assuming a concerted movement of all three hydrogen atoms[32c]. This process could also proceed via an intermediate dodecahedral structure (pathway k_3, Scheme 18), which is 10.3 and 13.1 kcal/mol above the ground state according to ab initio DFT and MP2 calculations for $OsH_5Cl(PH_3)_2$[29b] and $[OsH_5(PH_3)_3]^+$[33], respectively. Placement of a bulky ligand P^c into the A site of the dodecahedron contributes to the rise in energy.

The rearrangement between H_1, H_2, H_3 is facile because of the favorable geometry of the heavy-ligand skeleton, which is bent away from the hydrogen atoms (viewed from the centroid of the H_1, H_2, H_3 triangle).

Scheme 18

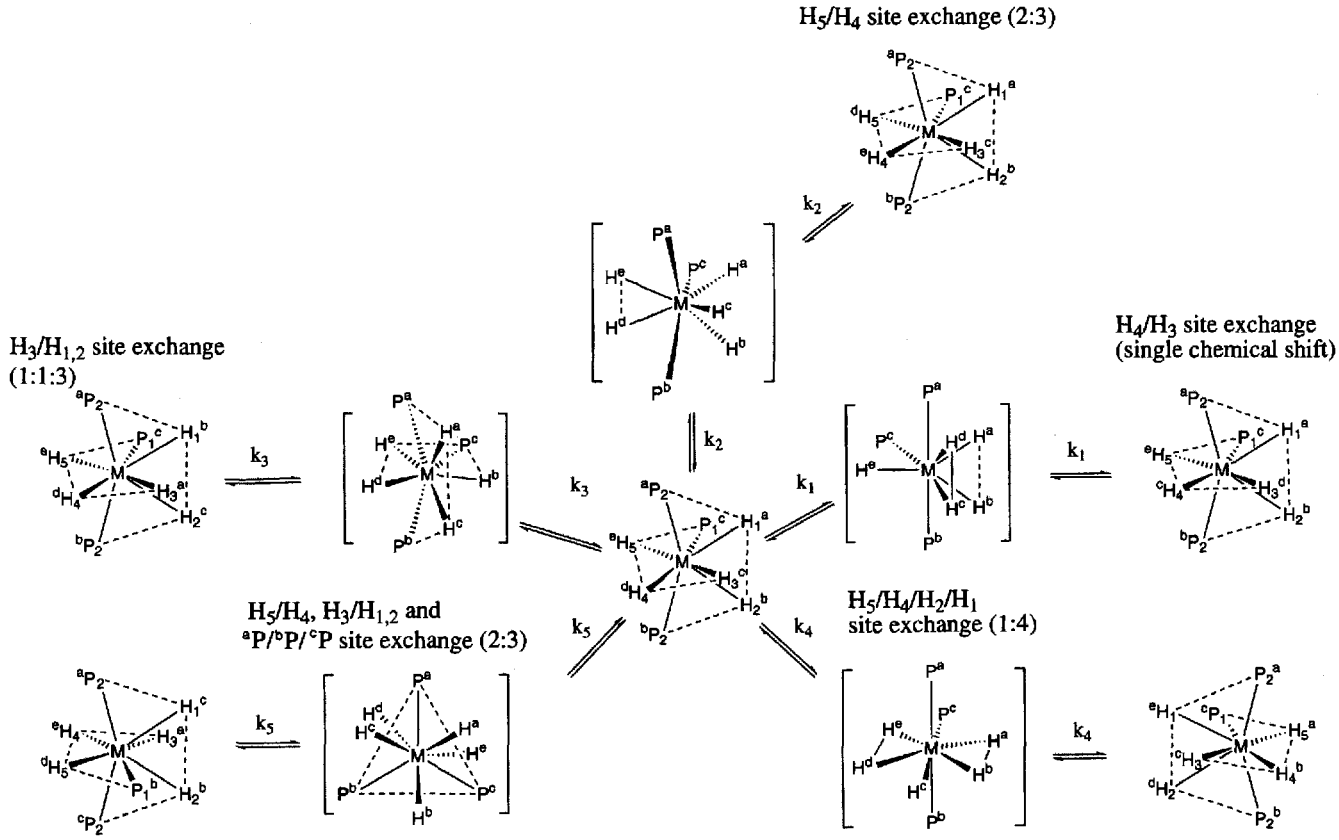

The observation of the 2:3 spectra for $Re(H)_5(AsEtPh_2)_3$ and $Re(H)_5(PMe_2Ph)_3$ requires exchange between sites 4 and 5 (H^e/H^d) at a rate $k_2 < k_3$. This must, however, be faster than the H_3/H_4 scrambling ($k_2 > k_1$). Under these circumstances hydrogen transfer between the $H_{1,2,3}$ and $H_{4,5}$ groups is avoided. The H_4/H_5 replacement can only proceed via the transition state structure given in Scheme 18 (pathway k_2). A crucial feature of this transformation is that the hydride H^c must be out of the plane formed by the heavy ligands and kept close to H^a and H^b. An alternative transient geometry (pathway k_4) with H^c in the plane of MP_3 would either result in a 1:4 pattern (if $k_4 > k_3$) or (in the present case with $k_3 > k_4$) completely average the chemical shifts to a single line. Apparently, the rate of the process k_4 (termed "pseudorotation"[32c]) must be slower than that of k_2 in $Re(H)_5(AsEtPh_2)_3$ and $Re(H)_5(PMe_2Ph)_3$. Avoidance of too close contacts with the phosphorus ligands might be one reason for H^c to stay away from the MP_3 plane. Another factor is that the interaction of H^c with the pair H^a and H^b is presumably attractive[30]. In the ab initio DFT and MP2 calculations the optimized transient structures of pathway k_4 were quite different, 9.9 and 32.9 kcal/mol above the ground state for $OsH_5Cl(PH_3)_2$[29b] and $[OsH_5(PH_3)_3]^+$[33], respectively. This result, if not influenced by the difference in computational methodology, would predict that the fluxional behavior may be substantially affected by the electronic properties of the heavy-ligand skeleton.

The **R**-type exchange between H_3 and H_4 in $Os(H_2)(H)_3X(PiPr_3)_2$ (pathway k_1) is suggested by the observation of the H_3-H_4 exchange coupling. This process also connects the two hydrogen "pools" $H_{1,2,3}$ and $H_{4,5}$ and establishes their mixing, and thus the averaging of the corresponding chemical shifts in the hydride region. Reaction step k_1 of Scheme 18 is connected with an intermediate, which is 6.2 and 17.7 kcal/mol above the ground state (as derived from the ab initio calculations) for $OsH_5Cl(PH_3)_2$ and $[OsH_5(PH_3)_3]^+$, respectively.

Finally, the ^{31}P-NMR exchange in $MH_5(PR_3)_3$ can be explained on the basis of ligand migration along the pathway k_5. The observed behavior is very similar to the ^{31}P-NMR exchange in $Os(H)_4L_3$ (Scheme 5). Since P^a, P^b, and P^c become equivalent at some point during the rearrangement, any of these ligands may end up in the $M-H_3-H_4-H_5$ mirror plane of the resulting ground state structure. Coalescence of the chemical shifts in this case does not require physical site exchange between the phosphanes. The observation[30] mentioned above of an AB_2 phosphorus and a 2:3 hydride spectrum of $Re(H)_5(PMe_2Ph)_3$ (at the same temperature, $-60\,^\circ C$) proves that $k_5 > k_2$. "Spinning" of the H^e-H^d pair is faster than the ligand migration described by k_5.

These considerations on the fluxionality of $MH_5L'L_2$ complexes complete our review on phosphane-substituted polyhydrides with Re, Fe, Ru, Os, and Ir metal centers. The

selection of examples demonstrates that a profound understanding of the structures of fluxional hydride complexes can only be accomplished on the basis of studies of the mechanistic features of their dynamics in solution. Dynamic characterization of hydride complexes may require extensive variable-temperature multinuclear NMR investigations down to the lowest attainable temperature (presently ca. −140 °C in $CDFCl_2/CDF_2Cl$), but will most certainly pay off for these efforts by providing fascinating structurally-significant insights. The attempted systematic approach of the present work is hoped to be useful for future mechanistic interpretations of the dynamic behavior of various transition metal polyhydrides.

[1] [1a] *Transition Metal Hydrides* (Ed.: E. L. Muetterties), Dekker, New York, **1971**. – [1b] *Dynamic Nuclear Magnetic Resonance Spectroscopy* (Eds.: L. M. Jackman, F. A. Cotton), Academic Press, New York, **1974**. – [1c] D. Moore, S. D. Robinson, *Chem. Soc. Rev.* **1983**, *12*, 415. – [1d] G. G. Hlatky, R. H. Crabtree, *Coord. Chem. Rev.* **1985**, *65*, 1. – [1e] G. J. Kubas, *Acc. Chem. Res.* **1988**, *21*, 129. – [1f] P. G. Jessop, R. H. Morris, *Coord. Chem. Rev.* **1992**, *121*, 155. – [1g] R. H. Crabtree, *Angew. Chem.* **1993**, *105*, 828; *Angew. Chem. Int. Ed. Engl.* **1993**, *32*, 789. – [1h] D. M. Heinekey, W. J. Oldham, *Chem. Rev.* **1993**, *93*, 913.

[2] [2a] F. N. Tebbe, P. Meakin, J. P. Jesson, E. L. Muetterties, *J. Am. Chem. Soc.* **1970**, *92*, 1068. – [2b] P. Meakin, L. J. Guggenberger, J. P. Jesson, D. H. Gerlach, F. N. Tebbe, W. G. Peet, E. L. Muetterties, *J. Am. Chem. Soc.* **1970**, *92*, 3482. – [2c] J. P. Jesson, E. L. Muetterties, P. Meakin, *J. Am. Chem. Soc.* **1971**, *93*, 5261. – [2d] P. Meakin, E. L. Muetterties, F. N. Tebbe, J. P. Jesson, *J. Am. Chem. Soc.* **1971**, *93*, 4701. – [2e] P. Meakin, E. L. Muetterties, J. P. Jesson, *J. Am. Chem. Soc.* **1972**, *94*, 5271. – [2f] P. Meakin, E. L. Muetterties, J. P. Jesson, *J. Am. Chem. Soc.* **1973**, *95*, 75. – [2g] P. Meakin, L. J. Guggenberger, W. G. Peet, E. L. Muetterties, J. P. Jesson, *J. Am. Chem. Soc.* **1973**, *95*, 1467.

[3] [3a] M. Mediati, G. N. Tachibana, C. M. Jensen, *Inorg. Chem.* **1990**, *29*, 3. – [3b] D. G. Gusev, V. I. Bakhmutov, V. V. Grushin, M. E. Vol'pin, *Inorg. Chim. Acta* **1990**, *177*, 115. – [3c] M. Mediati, G. N. Tachibana, C. M. Jensen, *Inorg. Chem.* **1992**, *31*, 1827. – [3d] A. Albinati, V. I. Bakhmutov, K. G. Caulton, E. Clot, J. Eckert, O. Eisenstein, D. G. Gusev, V. V. Grushin, B. E. Hauger, W. Klooster, T. F. Koetzle, R. K. McMullan, T. J. O'Loughlin, M. Pelissier, J. S. Ricci, M. P. Sigalas, A. B. Vymenits, *J. Am. Chem. Soc.* **1993**, *115*, 7300. – [3e] T. Le-Husebo, C. M. Jensen, *Inorg. Chem.* **1993**, *32*, 3797. – [3f] B. E. Hauger, D. G. Gusev, K. G. Caulton, *J. Am. Chem. Soc.* **1994**, *116*, 208.

[4] [4a] G. J. Kubas, C. J. Burns, J. Eckert, S. W. Johnson, A. C. Larson, P. J. Vergamini, C. J. Unkefer, G. R. K. Khalsa, S. A. Jackson, O. Eisenstein, *J. Am. Chem. Soc.* **1993**, *115*, 569. – [4b] J. Eckert, C. M. Jensen, T. F. Koetzle, T. L. Husebo, J. Nicol, P. Wu, *J. Am. Chem. Soc.* **1995**, *117*, 7271. – [4c] G. J. Kubas, J. E. Nelson, J. C. Bryan, J. Eckert, L. Wisniewski, K. W. Zilm, *Inorg. Chem.* **1994**, *33*, 2954.

[5] V. I. Bakhmutov, T. Burgi, H. Berke, *Organometallics* **1994**, *13*, 4203.

[6] D. G. Gusev, D. Nietlispach, A. V. Vymenits, V. I. Bakhmutov, H. Berke, *Inorg. Chem.* **1993**, *32*, 3270.

[7] [7a] D. G. Gusev, R. Kuhlman, G. Sini, O. Eisenstein, K. G. Caulton, *J. Am. Chem. Soc.* **1994**, *116*, 2685. – [7b] E. Clot, C. Leforestier, O. Eisenstein, M. Pélissier, *J. Am. Chem. Soc.* **1995**, *117*, 1797.

[8] A. Jarid, M. Moreno, A. Lledós, J. M. Lluch, J. Bertrán, *J. Am. Chem. Soc.* **1995**, *117*, 1069.

[9] D. W. Hart, R. Bau, T. F. Koetzle, *J. Am. Chem. Soc.* **1977**, *99*, 7557.

[10] J. W. Bruno, J. C. Huffman, M. A. Green, J. D. Zubkowski, W. E. Hatfield, K. G. Caulton, *Organometallics* **1990**, *9*, 2556.

[11] [11a] D. G. Gusev, D. Nietlispach, I. L. Eremenko, H. Berke, *Inorg. Chem.* **1993**, *32*, 3628. – [11b] W. D. Jones, J. A. Maguire, *Organometallics* **1987**, *6*, 1728.

[12] [12a] M. Aracama, M. A. Esteruelas, F. J. Lahoz, J. A. Lopez, U. Meyer, L. A. Oro, H. Werner, *Inorg. Chem.* **1991**, *30*, 288. – [12b] D. G. Gusev, R. Kuhlman, J. R. Rambo, H. Berke, O. Eisenstein, K. G. Caulton, *J. Am. Chem. Soc.* **1995**, *117*, 281.

[13] [13a] H. Werner, M. A. Esteruelas, U. Meyer, B. Wrackmeyer, *Chem. Ber.* **1987**, *120*, 11. – [13b] M. A. Esteruelas, C. Valero, L. A. Oro, U. Meyer, H. Werner, *Inorg. Chem.* **1991**, *30*, 1159. – [13c] J. Espuelas, M. A. Esteruelas, F. J. Lahoz, L. A. Oro, C. Valero, *Organometallics* **1993**, *12*, 663. – [13d] D. G. Gusev, A. B. Vymenits, V. I. Bakhmutov, *Inorg. Chim. Acta* **1991**, *179*, 195. – [13e] D. G. Gusev, A. B. Vymenits, V. I. Bakhmutov, *Inorg. Chem.* **1992**, *31*, 1. – [13f] D. G. Gusev, R. L. Kuhlman, K. B. Renkema, O. Eisenstein, K. G. Caulton, *Inorg. Chem.* **1996**, in press.

[14] L. L. Wisniewski, M. Mediati, C. M. Jensen, K. W. Zilm, *J. Am. Chem. Soc.* **1993**, *115*, 7533.

[15] [15a] B. Chin, A. J. Lough, R. H. Morris, C. T. Schweitzer, C. D'Agostino, *Inorg. Chem.* **1994**, *33*, 6278. – [15b] Another example is ref.[3d].

[16] D. G. Gusev, R. Hübener, P. Burger, O. Orama, H. Berke, *J. Am. Chem. Soc.* **1996**, submitted.

[17] A. R. Siedle, R. A. Newmark, L. H. Pignolet, *Inorg. Chem.* **1986**, *25*, 3412.

[18] F. A. Cotton, R. L. Luck, *Inorg. Chem.* **1989**, *28*, 2181.

[19] H. Jacobsen, H. Berke, unpublished results.

[20] V. G. Albano, P. L. Bellon, *J. Organomet. Chem.* **1972**, *37*, 151.

[21] See, for example: [21a] J. S. Ricci, T. F. Koetzle, M. T. Bautista, T. M. Hofstede, R. H. Morris, J. F. Sawyer, *J. Am. Chem. Soc.* **1989**, *111*, 8823. – [21b] A. Hills, D. L. Hughes, M. Jimenez-Tenorio, G. J. Leigh, A. T. Rowley, *J. Chem. Soc., Dalton Trans.* **1993**, 3041.

[22] [22a] M. Ogasawara, M. Saburi, *J. Organomet. Chem.* **1994**, *482*, 7. – [22b] A. P. Ginsberg, M. E. Tully, *J. Am. Chem. Soc.* **1973**, *95*, 4749.

[23] [23a] M. Saburi, K. Aoyagi, T. Kodama, T. Takahashi, Y. Uchida, K. Kozawa, T. Uchida, *Chem. Lett.* **1990**, 1909. – [23b] A. Mezzetti, A. DelZotto, P. Rigo, E. Farnetti, *J. Chem. Soc., Dalton Trans.* **1991**, 1525.

[24] [24a] M. A. Esteruelas, E. Sola, L. A. Oro, U. Meyer, H. Werner, *Angew. Chem.* **1988**, *100*, 1621; *Angew. Chem. Int. Ed. Engl.* **1988**, *27*, 1563. – [24b] A. Andriollo, M. A. Esteruelas, U. Meyer, L. A. Oro, R. A. Sanchez-Delgado, E. Sola, C. Valero, H. Werner, *J. Am. Chem. Soc.* **1989**, *111*, 7431.

[25] [25a] X.-L. Luo, R. H. Crabtree, *J. Chem. Soc., Chem. Commun.* **1990**, 189. – [25b] X.-L. Luo, R. H. Crabtree, *J. Am. Chem. Soc.* **1990**, *112*, 6912.

[26] D. M. Lunder, M. A. Green, W. E. Streib, K. G. Caulton, *Inorg. Chem.* **1989**, *28*, 4527.

[27] A computational study failed to reinterpret the experimental NMR data and to reproduce the structural features of the $[Re(H_2)(H)_2(CO)(PR_3)_3]^+$ complexes: Z. Lin, M. B. Hall, *J. Am. Chem. Soc.* **1994**, *116*, 4446.

[28] [28a] L. S. Van Der Sluys, J. Eckert, O. Eisenstein, J. H. Hall, J. C. Huffman, S. A. Jackson, T. F. Koetzle, G. J. Kubas, P. J. Vergamini, K: G. Caulton, *J. Am. Chem.Soc.* **1990**, *112*, 4831. – [28b] F. Maseras, M. Duran, A. Lledós, J.Bertrán, *J. Am. Chem. Soc.* **1991**, *113*, 2879. – [28c] F. Maseras, M. Duran, A. Lledós, J. Bertrán, *J. Am. Chem. Soc.* **1992**, *114*, 2922.

[29] [29a] D. G. Gusev, V. F. Kuznetsov, I. L. Eremenko, H. Berke, *J. Am. Chem. Soc.* **1993**, *115*, 5831. – [29b] R. Kuhlman, D. G. Gusev, O. Eisenstein, K. G. Caulton, manuscript in preparation.

[30] T. J. Emge, T. F. Koetzle, J. W. Bruno, K. G. Caulton, *Inorg. Chem.* **1984**, *23*, 4012.

[31] T. J. Johnson, A. Albinati, T. F. Koetzle, J. Ricci, O. Eisenstein, J. H. Huffman, K. G. Caulton, *Inorg. Chem.* **1994**, *33*, 4966.

[32] [32a] A. P. Ginsberg, S. C. Abrahams, P. B. Jamieson, *J. Am. Chem. Soc.* **1973**, *95*, 4751. – [32b] F. A. Cotton, R. L. Luck, *J. Am. Chem. Soc.* **1989**, *111*, 5757. – [32c] J. C. Lee, Jr., W. Yao, R. H. Crabtree, H. Rüegger, *Inorg. Chem.* **1996**, *35*, 695.

[33] F. Maseras, N. Koga, K. Morokuma, *J. Am. Chem. Soc.* **1993**, *115*, 8313.

[96084]